J Mol Model (2013) 19:383–390
DOI 10.1007/s00894-012-1557-2

ORIGINAL PAPER

Sequence selectivity of azinomycin B in DNA alkylation and cross-linking: a QM/MM study

Dhurairajan Senthilnathan · Anbarasan Kalaiselvan · Ponnambalam Venuvanalingam

Received: 29 March 2012 / Accepted: 1 August 2012 / Published online: 24 August 2012

Abstract Azinomycin B—a well-known antitumor drug—forms cross-links with DNA through alkylation of purine bases and blocks tumor cell growth. This reaction has been modeled using the ONIOM (B3LYP/6-31+g(d):UFF) method to understand the mechanism and sequence selectivity. ONIOM results have been checked for reliability by comparing them with full quantum mechanics calculations for selected paths. Calculations reveal that, among the purine bases, guanine is more reactive and is alkylated by aziridine ring through the C10 position, followed by alkylation of the epoxide ring through the C21 position of Azinomycin B. While the mono alkylation is controlled kinetically, bis-alkylation is controlled thermodynamically. Solvent effects were included using polarized-continuum-model calculations and no significant change from gas phase results was observed.

Keywords Azinomycin B · Antitumor activity · Cross-link mechanism · QM/MM study · Density functional theory

Introduction

Azinomycin A and azinomycin B are antitumor agents that exhibit both in vitro cytotoxic activity and in vivo antitumor activity. They have a functionalized structure containing aziridino [1, 2] pyrrolidine and labile epoxide rings. The biological activity [1–5] of azinomycin B is due to the formation of covalent interstrand cross-links with the purine bases of duplex DNA within the major groove. This covalent interaction [6, 7] occurs only at the replication fork region of DNA, and the selective binding of azinomycin B with DNA damages the DNA of tumor cells. An interstrand covalent linkage arises between the electrophilic aziridine and epoxide rings of azinomycin B and the purine bases viz., adenine and guanine. The cross-linking takes place via an alkylation mechanism through the C21 and C10 carbons of azinomycin B and the N7 position of the purine bases that results in ring cleavage [8, 9]. The chemical instability and limited natural sources of these agents have slowed down the detailed investigation of their biological evolution [10].

Through conformational studies, Coleman and Alcaro [11] suggested a mechanism of cross-linking through alkylation of adenosine by the bottom aziridine (C10) followed by alkylation of guanosine by the top epoxide (C21). They also reported the comparative strengths of antitumor activity of azinomycin B and its analogues. They observed the highest level of inter-system crossing (ISC) with the 5′-d(*G*CC)-3′/3′-d(CG*G*)-5′ base sequence (italicized bases indicate sites of reaction) and suggested that initial alkylation occurs on the more nucleophilic 3′-d(CG*G*)-5′ strands by kinetic experiments [12]. LePla et al. [13] have reported through phosphorimage analysis that the mono alkylation and intersystem cross-linking (bis-alkylation) of DNA with azinomycin B occurred through the guanine nucleobase. Recently, Gossens et al. [14] reported that N7 of guanine is more reactive than the adenine N7 in the antitumor approach to targeting DNA with organometallic drugs. Although several experimental [15, 16] and molecular modeling [11, 17–19] studies have concluded that azinomycin B acts as an antitumor agent by covalent alkylation and by cross-linking with DNA, the mechanism of this reaction, and the sequence selectivity of azinomycin B needs further investigation; this requires a detailed electronic

Electronic supplementary material The online version of this article (doi:10.1007/s00894-012-1557-2) contains supplementary material, which is available to authorized users.

D. Senthilnathan · P. Venuvanalingam (✉)
School of Chemistry, Bharathidasan University,
Tiruchirappalli 620024, India
e-mail: venuvanalingam@yahoo.com

A. Kalaiselvan
Department of Chemistry, Anna University of Technology,
Tiruchirappalli, Thirukkuvalai Campus,
Thirukkuvalai 610 204, Tamil Nadu, India

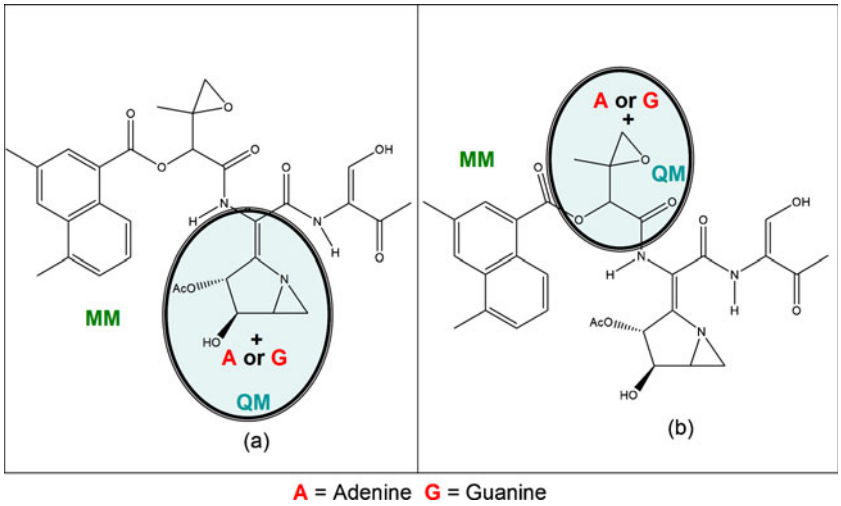

Fig. 1 Pictorial representation of quantum mechanics (QM) and molecular mechanics (MM) layer selection for the alkylation of the **a** aziridine or **b** epoxide ring of azinomycin B

structure analysis. Considering all these observations, and to obtain a better understanding of the chemical events underlying the biological activity of azinomycin B heterocyclic rings, we planned to model the cross-linking reaction of DNA

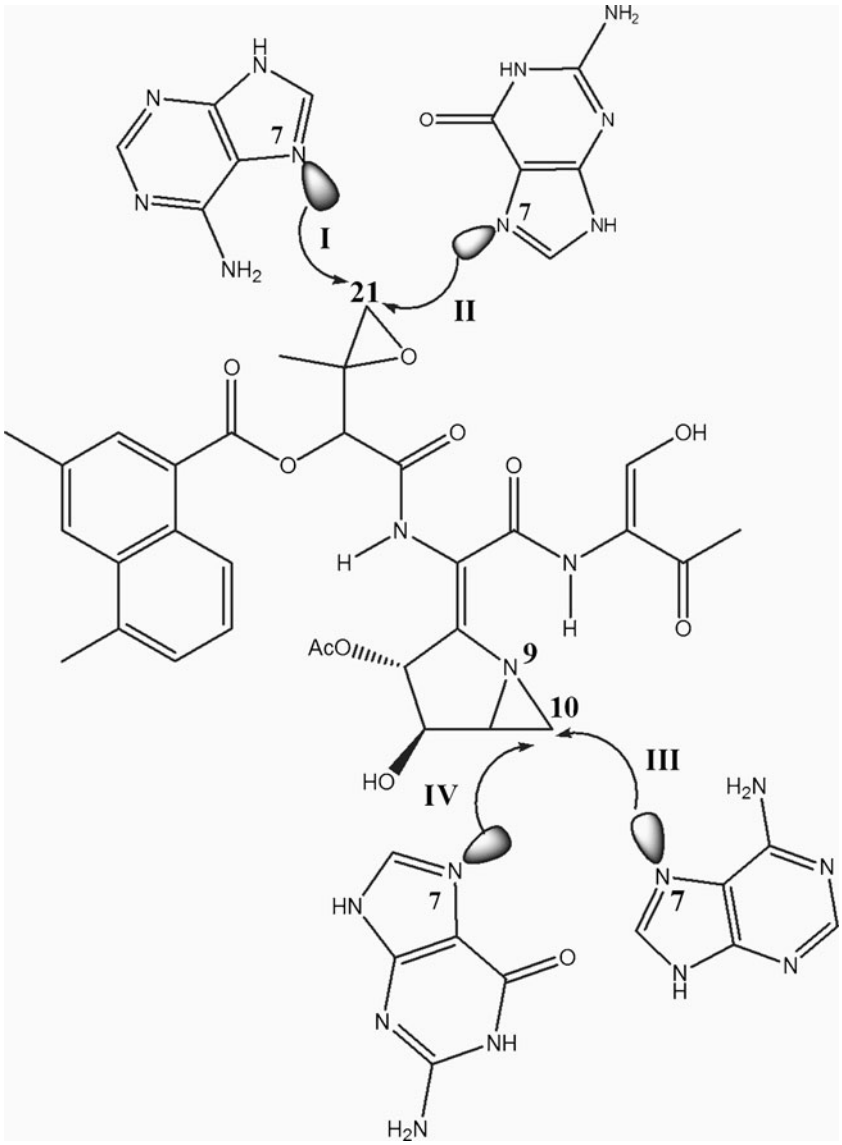

Fig. 2 Different pathways of mono-alkylation of purine bases by epoxide and aziridine rings of azinomycin B

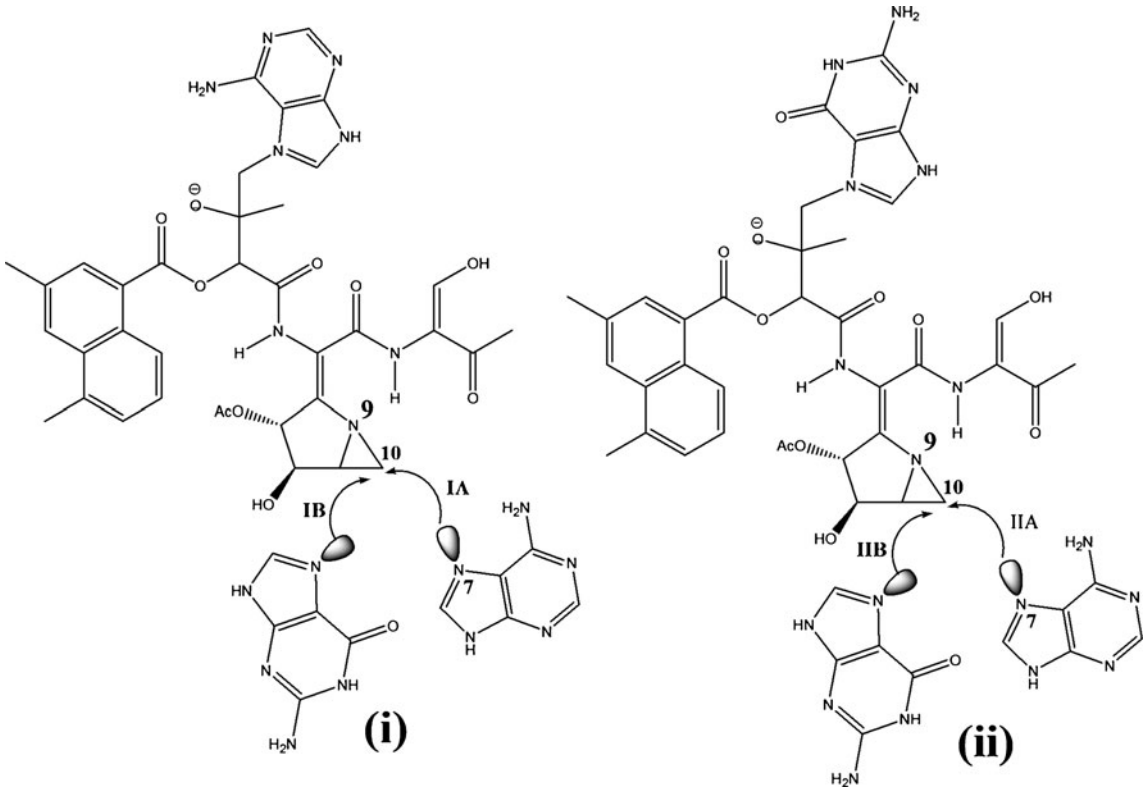

Fig. 3 Different pathways (IA, IB, IIA and IIB) of bis-alkylation reaction on the aziridine ring of mono-alkylated azinomycin B with (i) adenine, (ii) guanine

with azinomycin B through purine bases with the following objectives: (1) to find the relative order of reactivity of DNA purine bases in mono-alkylation by azinomycin B; and (2) to determine the order of reactivity between epoxide or azirdine

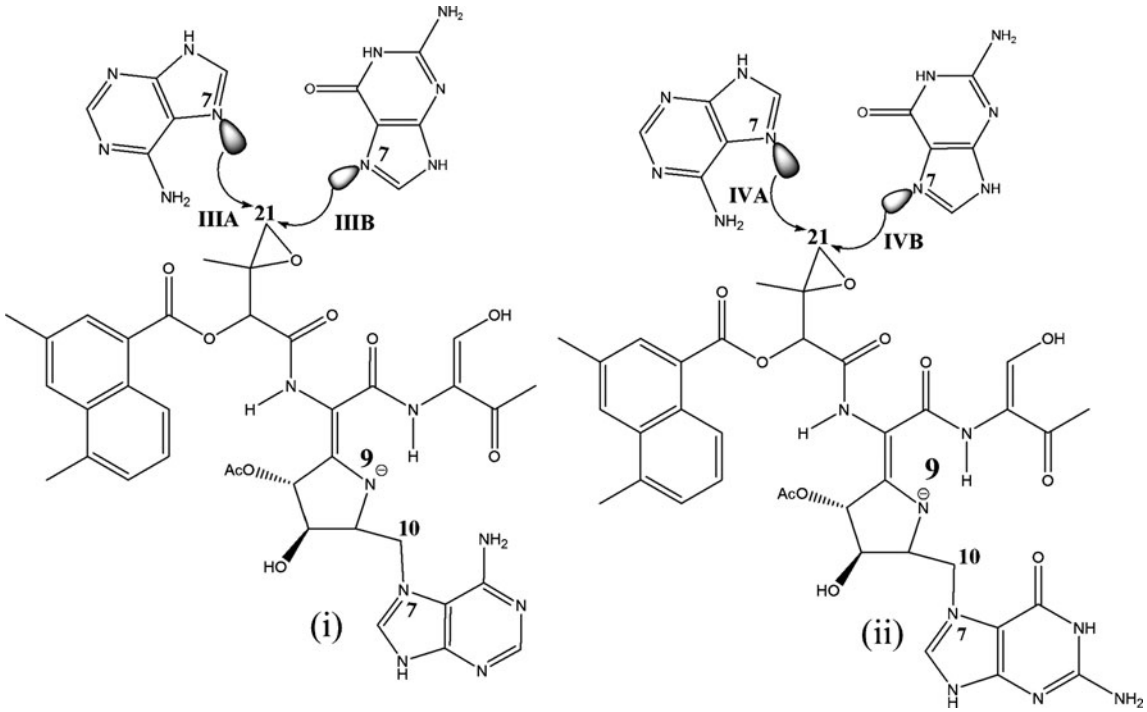

Fig. 4 Different pathways (IIIA, IIIB, IVA and IVB) of bis-alkylation reaction on the epoxide ring of mono-alkylated azinomycin B with (i) adenine, (ii) guanine

figure of azinomycin A and B with purine bases in DNA. These questions are vital in the investigation of DNA cross-linking by azinomycin B in alkylation mode.

Computational details

Geometry optimizations were carried out using the hybrid quantum mechanics/molecular mechanics approach (QM/MM) (B3LYP/6-31+g(d):UFF) available in ONIOM [20, 21]. All stationary points were characterized by computing vibrational frequencies. Transition states were further confirmed by harmonic analysis and by intrinsic reaction coordinates (IRC). All computations were performed using the Guassian03 program [20, 21]. The azinomycin B drug is active with DNA purine bases only at the replication fork area of DNA. In the replication fork, the purine bases of DNA have no geometrical constraint, so move freely and behave as isolated bases due to the dynamic mobility of single strand of DNA. Therefore, the reductionistic approach was followed by considering the significant reactive parts of azinomycin B, i.e., aziridine and epoxide rings with purine bases as the QM region and the rest of azinomycin B as the MM region as illustrated in Fig. 1. In order to check the reliability of QM/MM calculations, full QM calculations were performed at B3LYP/6-31g(d) level for selected paths—mono-alkylation paths (III and IV) and bis-alkylation paths—and both values were in reasonable agreement. Solvent effects (water, $\varepsilon=80$) were modeled by the polarized-continuum-model (PCM), on B3LYP/6-31+g(d) optimized structures. Topological analysis according to Bader's quantum theory of atoms in molecules (AIM) was carried out for adenine and guanine

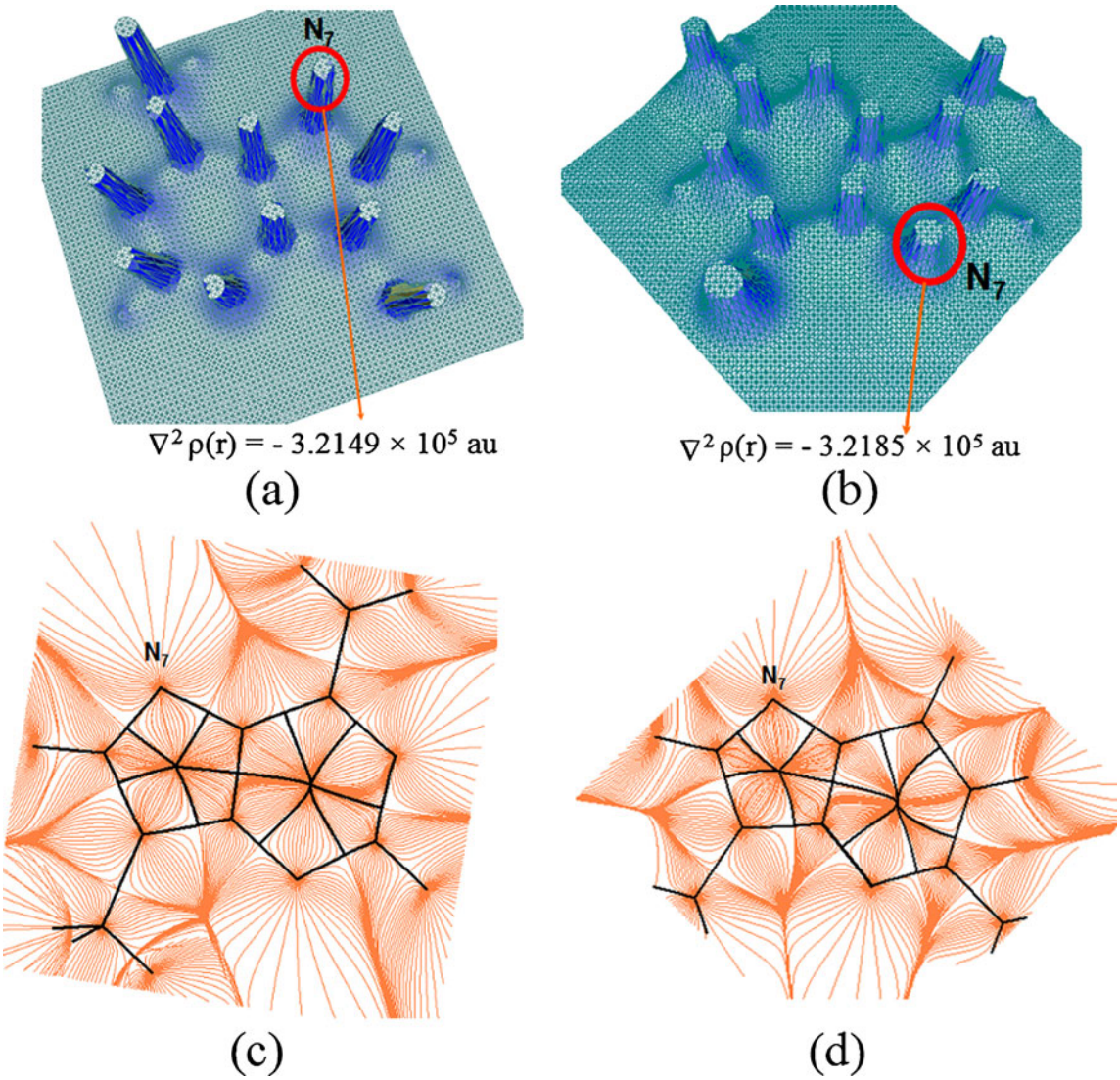

Fig. 5 Electron density relief map of adenine (**a**) and guanine (**b**) with Laplacian values. **c**, **d** Trajectory plot of gradient victor field of the charge density of adenine (**c**) and guanine (**d**). In the trajectory plots *black solid lines* denotes bond paths and critical point paths

at B3LYP/6-31+g(d) level using AIM2000 [22–25]. Second order perturbation energy analysis was also carried out for transition state structures at B3LYP/6-31+g(d) level using Nnatural bond order (NBO) analysis. Natural population analysis (NPA) charges were computed to examine the site selectivity for nucleophilic attack by azinomycin B.

Results and discussion

Cross-linking of azinomycin B with DNA purine bases takes place by an alkylation mechanism that occurs in two steps, namely mono-alkylation and bis-alkylation. The detailed reaction schemes with different possible approaches of purine bases with azinomycin B are presented in Figs. 2, 3, 4.

The computed electrostatic potential map of azinomycin B shows a positive potential at carbons C10 and C21. The NPA charges of azinomycin B computed at the B3LYP/6-31+g(d)level reveals that the C21 (0.31) and C10 (0.56) positions are electrophilic and are highly susceptible to the attack of nucleophilic purine bases; this is in agreement with earlier reports [12–14].

Hence, the cross-linking of azinomycin B depends on the electrophilicity of azinomycin B heterocyclic rings and the localization of electron density in purine bases. To determine the charge localization of purine bases, topological analysis was performed. The Laplacian electron density (relief map) of adenine (Fig. 5a) and guanine (Fig. 5b) are represented in Fig. 5 witha trajectory plot of the gradient vector field of the charge density of adenine (Fig. 5c) and guanine (Fig. 5d).

The negative $\nabla^2\rho(r)$ values of all the atoms in purine bases show that the electron density is concentrated locally around the nitrogen atoms (see Supporting information). The higher negative $\nabla^2\rho(r)$ value of N7 of adenine and guanine reveal that alkylation takes place only at the N7 position. The relatively lower negative electron density value $\nabla^2\rho(r)$ of adenine N7 compared to guanine N7 reveals that the nucleophilicity of guanine N7 is higher and is alkylated first.

The gradient trajectory plot of adenine (Fig. 5c) and guanine (Fig. 5d) shows the electron density distribution and zero flux of the gradient vector at bond critical points (BCPs). The deviation of zero flux charge density at the BCP of N7 and the neighboring carbon bond (Fig. 5d) of guanine is relatively high compared to the BCP of adenine N7 with the neighboring carbon bond (Fig. 5c), and this implies that the localization of electron density at N7 of guanine is high compared to that of N7 of adenine.

Activation and reaction free energies of various possible pathways of the alkylation reactions listed in Table 1 show that alkylation of guanine N7 (IV) is relatively more favorable than adenine N7 (III) by the aziridine ring of azinomycin B, and that they are controlled kinetically. Frontier orbital energies also reflect the same trend. Very high activation energies clearly rule out alkylation through the epoxide ring (I and II). Moreover, the activation energies of bis-alkylation of mono-alkylated purine bases by aziridine ring, i.e., pathways IA, IB, II A and IIB (Fig. 4) are very high, confirming that mono-alkylation of purine bases by the epoxide ring is not a favorable path. The high exothermicity of the reaction is due to the release of aziridine ring strain.

Table 1 Activation and reaction free energies (kcal mol^{-1}) of various pathways of mono- and bis-alkylation of purine bases by azinomycin B at ONIOM (B3LYP/6-31+G(d):UFF) level. Full quantum mechanics (QM) calculations at B3LYP/6-31+G(d,p) values are given in parentheses

Reaction	Pathway	$\Delta G^{\ddagger}$	ΔG_r
Mono-alkylation	I	37.52	−18.96
	II	34.29	−10.16
	III	20.57 (19.06)	−13.55 (−12.82)
	IV	18.07 (17.31)	−9.21 (−10.03)
Bis-alkylation	IA	31.59	−36.70
	IB	27.25	−42.34
	IIA	40.50	−13.94
	IIB	36.10	−21.42
	IIIA	32.96	−38.05
	IIIB	23.91	−42.54
	IVA	35.31 (34.02)	−12.27 (−13.68)
	IVB	30.83 (28.99)	−39.98 (−40.62)

In order to check the reliability of the chosen QM/MM method, the mono-alkylation and bis-alkylation pathways were modeled at full quantum chemical method using B3LYP/6-31+g(d,p) level for selected paths. The computed relative free energies at this level are given in parantheses in Table 1. The values show that the QM/MM method slightly underestimates the activation barrier, while it slightly overestimates the reaction energy. PCM calculation results are presented in the Supporting information (ST1). The inclusion of solvent effects has not altered the free energy profiles and hence does not affect the selectivity.

In general, calculations predict that, if the mono-alkylation is a kinetically controlled reaction, guanine will be alkylated first by aziridine bottom, and if it is thermodynamically controlled, adenine will be alkylated first by aziridine bottom. The activation free energy difference between mono alkylation of adenine and guanine by the aziridine ring of azinomycin B is found to be 2.50 kcal mol^{-1}, which is very low and hence it is difficult to draw any conclusion about the relative order of reactivity of the purine bases. However, the FMO energy difference between the guanine N7 lone pair orbital and LUMO of azinomycin B is 3.56 eV, while it is 3.90 eV for the adenine N7 lone pair

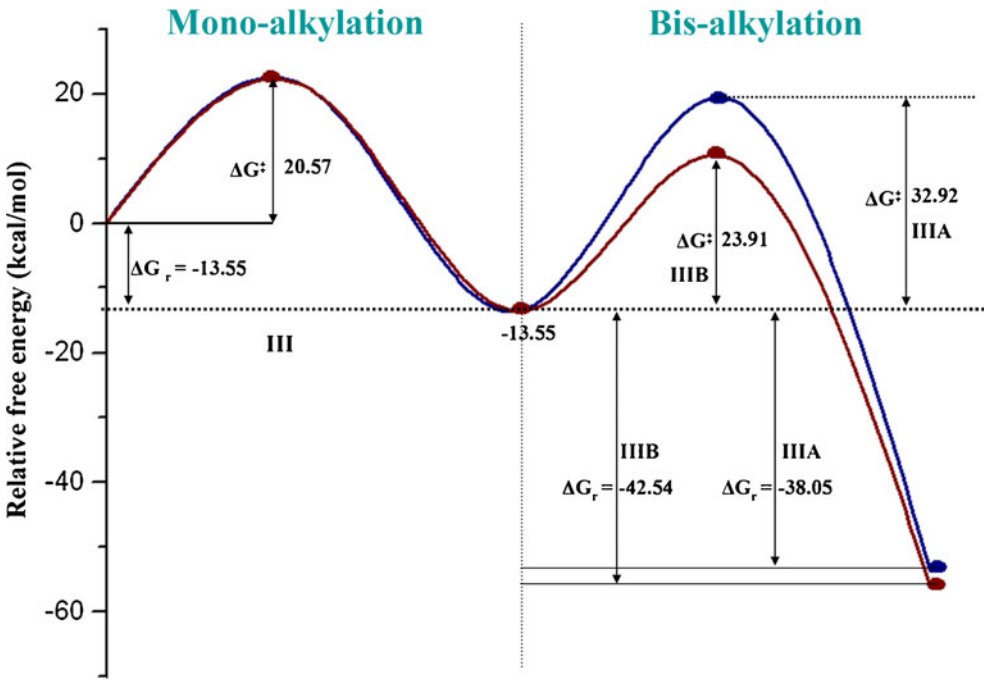

Fig. 6 Relative free energy profile of mono-alkylation of adenine (III) by the aziridine ring followed by bis-alkylation of adenine (IIIA) and guanine (IIIB) by the epoxide ring of azinomycin B

orbital and LUMO of azinomycin B (see Supporting information). This energy gap (7.84 kcal mol^{-1}) can be taken as evidence for a stronger guanine–azinomycin B interaction than adenine–azinomycin B interaction. Also, topological analysis and electrostatic potential surfaces indicate a stronger guanine–azinomycin interaction. Further, second order perturbation energy analysis reveals that the interaction between the guanine N7 lone pair orbital and the σ* orbital of C10–N9 is stronger (120.65 kcal mol^{-1}) than the interaction between the adenine N7 lone pair orbital and the σ* orbital of C10–N9 (109.01 kcal mol^{-1}), confirming that the guanine and azinomycin B interaction is more favorable than the adenine and azinomycin B interaction. This is in excellent agreement with experimental observations [12, 13].

The free energy profile of the mono- and bis-alkylation of adenine and guanine by azinomycin-B are shown in Figs. 6 and 7, respectively.

In the mono-alkylated product, if guanine is alkylated by the aziridine ring (C10) of azinomycin B, then the bis-alkylation of purine bases may take place via epoxide ring (C21) cleavage through the IVA or IVB pathway (Fig. 7). Activation energies predict that reaction pathway IVB, i.e. the

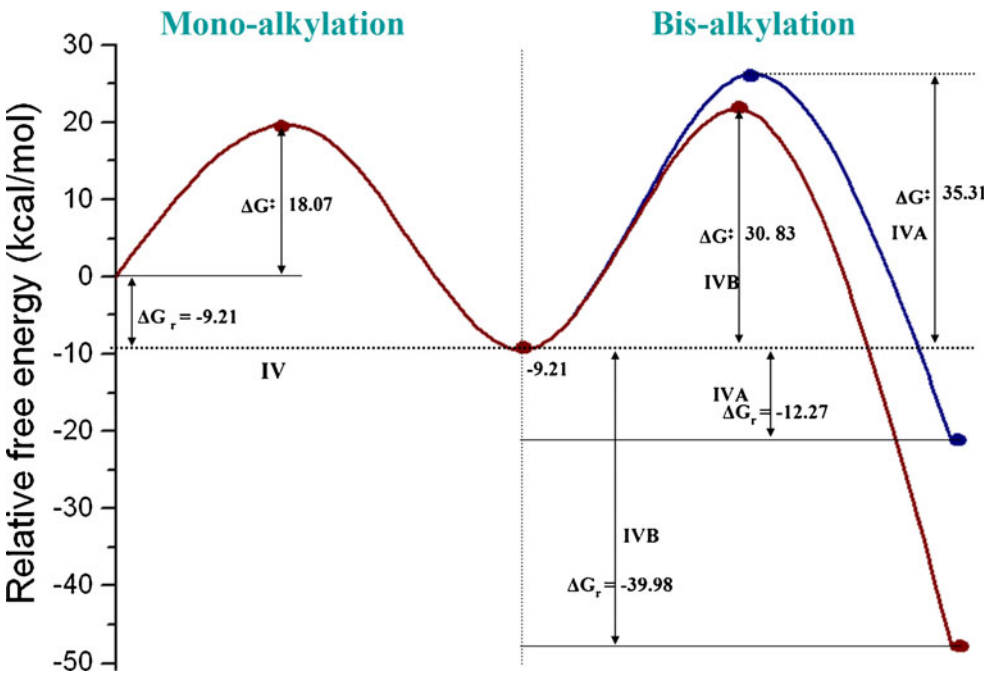

Fig. 7 Relative free energy profile of mono-alkylation of guanine (IV) by the aziridine ring followed by the bis-alkylation of adenine (IVA) and guanine (IVB) by the epoxide ring of azinomycin B

attack of the mono-alkylated product to guanine ,is energetically and electronically favored. Similarly, if adenine is alkylated in the mono-alkylation, IIIB is preferred over IIIA for the bis-alkylation (Fig. 6). In both cases (IIIB and IVB), the bis-alkylation reaction is both kinetically and thermodynamically controlled; finally, in the bis-alkylation step, also guanine is found to be more reactive than adenine, and path IIIB is the preferred reaction path (Fig. 8). The optimized structures of the transition states of the mono- and bis-alkylation reaction resemble an S_N2 type ring opening, i.e., the N7 of purine bases approaches the C10 and C21 positions from the back side.

Conclusions

Interaction of azinomycin B with DNA purine bases has been investigated by QM/MM methods available in ONIOM. The use of ONIOM methodology was validated by comparing with full QM calculations for selected paths. Computations reveal that (1) alkylation depends on the nucleophilicity of the purine bases in general and the N7 position of purine bases in particular. (2) FMO and topological analyses of purine bases prove that guanine is relatively more reactive than adenine. (3) Guanine N7 is alkylated first by the aziridine 'bottom' and then by epoxide 'top'. i.e., the nucleophilic guanine N7 reacts first with electrophilic C10 and then with C21 in the next step. (4) Mono-alkylation is controlled kinetically while the subsequent bis-alkylation is controlled both kinetically and thermodynamically. (5) Reaction path IIIB is kinetically and thermodynamically most preferred for bis-alkylation. (6) The aziridine and epoxide ring opening resembles an S_N2 mechanism. Computed NPA charges, electrostatic potential surfaces and second order perturbation analysis explain the attack of N7 with C10 and C21 positions very well. Solvent effects do not significantly alter the trends.

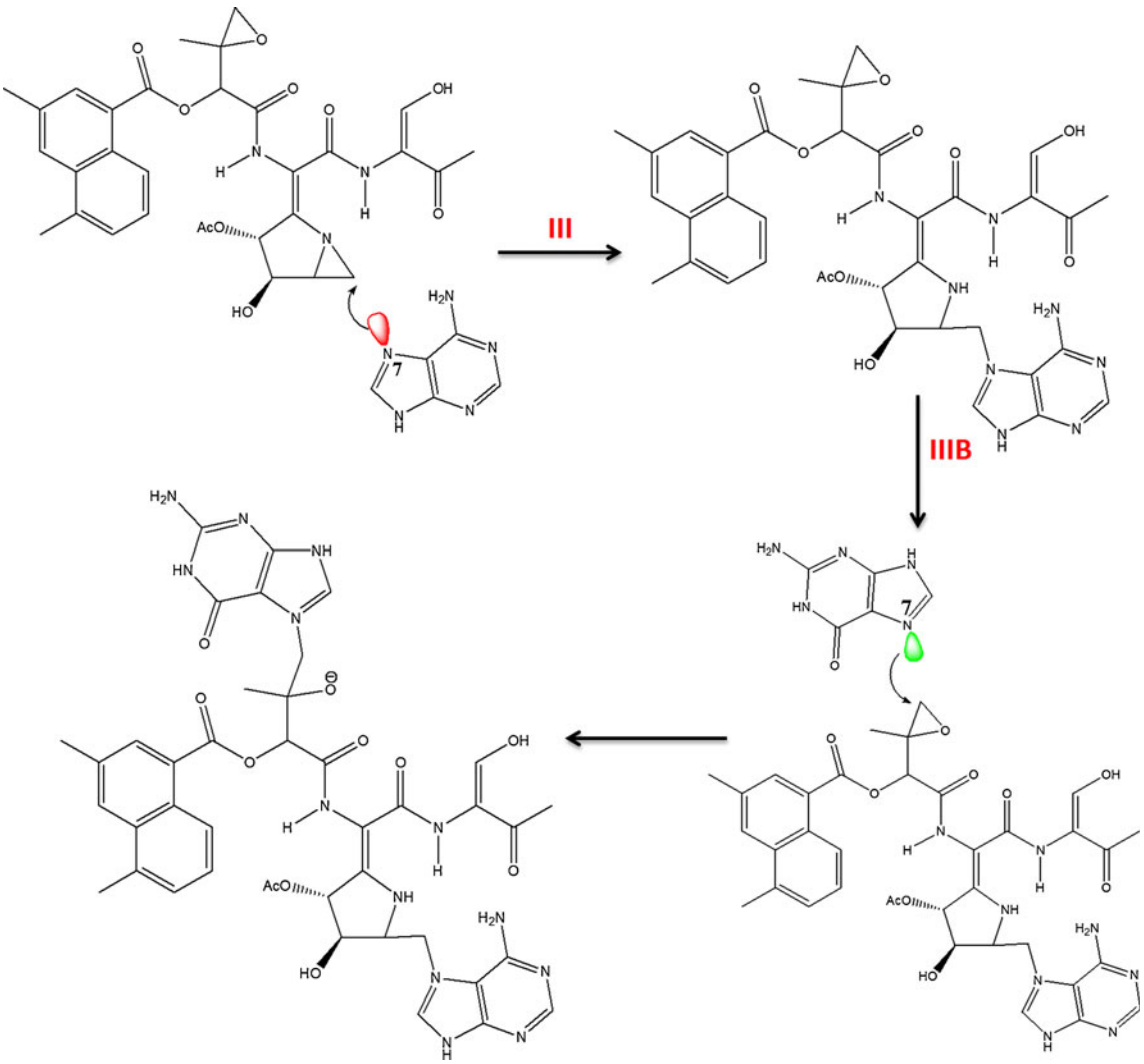

Fig. 8 Schematic representation of the favorable pathway of mono- and bis-alkylation of azinomycin B by adenine and guanine, respectively

Acknowledgments We thank the Council of Scientific and Industrial Research, India, for their financial support in the form of a research grant (Ref. No. 02(2158)/07/EMR-II). D.S. thanks the Council of Scientific and Industrial Research for financial support through a Senior Research Fellowship.

References

1. Nagaoka K, Matsumoto M, Oono J, Yokoi K, Ishizeki S, Nakashima T (1986) J Antibiot 39:1527–1532
2. Yokoi K, Nagaoka K, Nakashima T (1986) Chem Pharm Bull 34:4554–4561
3. Ishizeki S, Ohtsuka M, Irinoda K, Kukita KI, Nagoka T, Nakashima T (1987) J Antibiot 40:60–65
4. Hodgkinson TJ, Shipman M (2001) Tetrahedron 57:4467–4488
5. Hashimoto M, Matsumoto M, Yamada K, Terashima S (2003) Tetrahedron 59:3089–3097
6. Rajski SR, Williams RM (1998) Chem Rev 98:2723–2796
7. Hata T, Koga F, Sano Y, Kanamori K, Matsumae A, Sugawara R, Hoshi T, Shimi T, Ito S, Tomizawa S (1954) J Antibiot Ser A 7:107–112
8. Terawaki A, Greenberg J (1966) Nature 209:481–484
9. Hartley J, Hazrati A, Kelland L, Khanim R, Shipman M, Suzenet F, Walter L (2000) Angew Chem Int Ed 39:3467–3470
10. Ishizeki S, Ohtsuka M, Irinoda K, Kukita K, Nagaoka K, Nakashima T (1987) J Antibiot 40:60–65
11. Alcaro S, Coleman RS (2000) J Med Chem 43:2783–2788
12. Coleman RS, Perez RJ, Burk CH, Navarro CH (2002) J Am Chem Soc 124:13008–13017
13. LePla RC, Landreau CAS, Shipman M, Jones GDD (2005) Org Biomol Chem 3:1174–1175
14. Gossens C, Tavernelli I, Rothlisberger U (2009) J Phys Chem A 113:11888–11897
15. Armstrong RW, Salvati ME, Nguyen M (1992) J Am Chem Soc 114:3144–3145
16. Zang H, Gates KS (2000) Biochemistry 39:14968–14975
17. Alcaro S, Ortuso F, Coleman RS (2002) J Med Chem 45:861–870
18. Alcaro S, Coleman RS (1998) J Org Chem 63:4620–4625
19. Alcaro S, Francesco O, Coleman RS (2005) J Chem Inf Model 45:602–609
20. Dapprich S, Komiromi I, Byun KS, Morokuma K, Frisch MJ (1999) Theochem 1:461–462
21. Frisch MJ, Trucks GW, Schlegel HB, Scuseria GE, Robb MA, Cheeseman JR, Montgomery JA, Vreven T, Kudin KN, Burant JC, Millam JM, Iyengar SS, Tomasi J, Barone V, Mennucci B, Cossi M, Scalmani G, Rega N, Petersson GA, Nakatsuji H, Hada M, Ehara M, Toyota K, Fukuda R, Hasegawa J, Ishida M, Nakajima T, Honda Y, Kitao O, Nakai H, Klene M, Li X, Knox JE, Hratchian HP, Cross JB, Bakken V, Adamo C, Jaramillo J, Gomperts R, Stratmann RE, Yazyev O, Austin AJ, Cammi R, Pomelli C, Ochterski JW, Ayala PY, Morokuma K, Voth GA, Salvador P, Dannenberg JJ, Zakrzewski VG, Dapprich S, Daniels AD, Strain MC, Farkas O, Malick DK, Rabuck AD, Raghavachari K, Foresman JB, Ortiz JV, Cui Q, Baboul AG, Clifford S, Cioslowski J, Stefanov BB, Liu G, Liashenko A, Piskorz P, Komaromi I, Martin RL, Fox DJ, Keith T, Al-Laham MA, Peng CY, Nanayakkara A, Challacombe M, Gill PMW, Johnson B, Chen W, Wong MW, Gonzalez C, Pople JA (2004) Gaussian 03, Revision C02. Gaussian Inc, Wallingford
22. Bader RFW (1994) Atoms in molecules. A quantum theory. Clarendon, Oxford
23. Biegler-König F, Schönbohm J, Bayles DJ (2001) J Comput Chem 22:545–559
24. Kocher N, Henn J, Gostevskii B, Kost D, Kalikhman I, Engels B, Stalke D (2004) J Am Chem Soc 136:5563–5568
25. Henn J, Ilge D, Leusser D, Stalke D, Engels B (2004) J Phys Chem A 108:9442–9452